SeaWiFS measurements of the moon

Robert A. Barnes,† Robert E. Eplee, Jr., Frederick S. Patt

SAIC General Sciences Corporation, Laurel, MD 20707, USA, and
SeaWiFS Project, Code 970.2 NASA Goddard Space Flight Center, Greenbelt, MD 20771, USA

ABSTRACT

Measurements of the lunar surface in the visible and near infrared wavelength regions provide a new and intriguing method of determining changes in the sensitivities of Earth observing radiometers. Lunar measurements are part of the calibration strategy for the instruments in the Earth Observing System (EOS)[1] and part of the calibration strategy for the Sea Viewing Wide Field of View Sensor (SeaWiFS).[2,3] SeaWiFS was launched on August 1, 1997. The first SeaWiFS images of the Earth were taken on September 4, 1997, and the first lunar measurements were made on November 14, 1997. We describe the results from the initial nine lunar measurements by SeaWiFS, extending to July 10, 1998. The time series for the lunar images show changes in the sensitivities of SeaWiFS bands one through five (412 to 555 nm) to be very small over the eight month interval. For band 6 (670 nm), the decrease in sensitivity over seven months is ½%. For bands 7 and 8 (765 and 865 nm), the decreases are 1½% and 5% respectively. These changes, with reduced scatter in the results, are also found in the band ratios. The instrument changes can be seen in the SeaWiFS data products. Using the lunar time series, plus data from diffuser and ocean surface measurements, a time-dependent correction for the changes in the sensitivities of bands 6, 7, and 8 has been applied in the SeaWiFS data processing algorithm.

Keywords: SeaWiFS, ocean color, calibration, lunar calibration, measurement trends

1. INTRODUCTION

SeaWiFS[4] carries no onboard calibration standards. It has a diffuser panel that is used to measure the solar irradiance on a daily basis. However, the sun is viewed in a manner different from measurements of the Earth. The diffuser panel is not used for Earth measurements. It is an "extra" optical component used only to view the sun. SeaWiFS carries no device, such as a ratioing radiometer,[5] to measure changes in the diffuser's reflectance. Thus, using solar measurements only, it is not possible to separate changes in the reflectance of the diffuser from changes in the radiometric calibration of the sensor.

Since SeaWiFS is the sole scientific instrument onboard the SeaStar spacecraft (now called Orbview-2 by Orbital Sciences Corporation), it is possible to maneuver the spacecraft for SeaWiFS calibration purposes without compromising the operation of other instruments. Thus, once each month, SeaWiFS scans the moon at near full lunar phase. For the SeaWiFS mission, the moon is considered a reflecting surface that does not degrade[6] as does the instrument's solar diffuser. In addition, the rotation of the spacecraft for SeaWiFS scans of the moon allows lunar measurements to be made through the same optical train within the instrument as those for the Earth.

The SeaWiFS Project does not, at present, use the moon as an absolute radiometric standard for calibration purposes. The moon is used solely as a diffuse reflector whose surface remains unchanged. The lunar radiances viewed by SeaWiFS do change. Some of the radiance changes are due to geometric factors, such as the change in the Earth-sun distance over the course of a year. Other changes are due to the amount of the moon's surface that is viewed by SeaWiFS, such as changes linked to the lunar phase angle of the measurement. Still others are due to lunar libration,[7] which causes SeaWiFS to view a slightly different face of the moon from month to month. Over the course of a libration cycle, about 59% of the lunar surface can be seen from the Earth. These factors are discussed in Section 3.

Table 1 gives a list of the lunar measurements presented here. The table gives the dates and times of the measurements as well as the positions of the instrument when the measurements were taken. The spacecraft locations are given in Cartesian coordinates as the distance from the center of the Earth (in km). In Table 1, the Z direction is defined by the spin axis of the Earth, with +Z passing through the north pole. The X direction points toward the first point in Aries on the celestial

† For further author information -
R.A.B. (correspondence) email: rbarnes@calval.gsfc.nasa.gov; telephone: 301-286-0501; fax: 301-286-1775
R.E.E. email: eplee@calval.gsfc.nasa.gov
F.S.P. email: fred@sabalun.gsfc.nasa.gov

Table 1. Dates, Times, and Spacecraft Locations for the Initial Set of SeaWiFS Lunar Measurements. The spacecraf locations are given in km from the center of the Earth. See text for details.

	Time (UT)	Days After First Image	Spacecraft Location [X direction] (km)	Spacecraft Location [Y direction] (km)	Spacecraft Location [Z direction] (km)
Nov 14, 1997	22:50:09	71.27	4122.0	5569.9	1481.3
Dec 14, 1997	12:18:26	100.83	945.1	6757.2	1912.9
Jan 13, 1998	01:44:52	130.39	-2526.7	6418.1	1632.6
Feb 10, 1998	21:02:36	159.19	-5300.9	4452.4	1518.7
Mar 12, 1998	13:46:08	188.89	-6900.6	1243.0	1025.1
Apr 12, 1998	10:29:28	219.75	-6533.4	-2662.4	-692.8
May 12, 1998	01:33:05	249.38	-4295.4	-5498.8	-1265.3
Jun 10, 1998	13:18:49	278.87	-1021.3	-6823.1	-1638.3
Jul 10, 1998	01:04:02	308.36	2439.1	-6317.3	-2099.9

sphere, also known as the direction of the vernal equinox. The Y direction is defined from the right hand rule. This coordinate system is called J2000.

2. LUNAR IMAGE

SeaWiFS operates in a Sun synchronous orbit, crossing the Equator from north to south at local noon. In normal operation the spacecraft is maintained in a nadir orientation, using pitch-axis momentum wheels for attitude control, with a spacecraft pitch rate of 360° per orbit (about 0.06° per second). For lunar measurements, the rotation rate of the momentum wheels is increased, and the spacecraft is pitched in the opposite direction at a rate faster than the Earth view (0.15° per second). The maneuver is started past the South Pole passage and is timed such that SeaWiFS will view the moon as the spacecraft ground track passes the sub-lunar point. At the end of the maneuver, about 28 minutes later, when the spacecraft again points toward the Earth, the pitch rate is returned to normal. During views of the moon, the scan direction of SeaWiFS is such that the instrument scans across the lunar surface from west to east in celestial coordinates.

Since the moon appears to be a stationary object during SeaWiFS measurements, the number of scan lines in a lunar measurement depends upon the pitch rate of the instrument and the apparent size of the moon. The pitch maneuver causes SeaWiFS to over-sample the moon. There are approximately 25 scan lines of the moon in the lunar image (see Section 3.4), whereas the moon has a diameter that is equivalent to approximately 7 SeaWiFS samples.[3] The term “sample” is used here as a synonym for the word “pixel.” With a scan rate of six telescope rotations per second, the lunar image is collected in about four seconds.

A digital image of the moon is shown in Figure 1. It is the image for SeaWiFS band 1 for the first lunar measurement (November 14, 1997). The image gives the digital counts for each sample after the removal of the zero offset. The zero offset comes from a small, constant, internally-generated voltage that ensures that the digital counts in the data stream are always greater than zero. The top of the image (scan line 1) is north; the left side of the image is west (sample 1). The upper left hand sample is designated as scan line 1, sample 1 (1, 1); the lower right hand sample as scan line 33, sample 22 (33, 22). The central core of the lunar image includes all samples with counts greater than 1% of the maximum.

In Figure 1, the maximum is 735 counts. The drop off to zero counts at the top and bottom of the core of the image is approximately the same. There is no such symmetry on the left and right hand sides of the lunar image. This effect is due to stray light in the instrument and has been seen in laboratory testing of the instrument.[8] The moon is a very good target to examine the response of SeaWiFS to bright-to-dark and dark-to-bright transitions in the scenes that it measures.

The values in Figure 1 are given as digital counts. This form of the data gives the simplest presentation of the measurements. However, in the SeaWiFS calibration algorithm, the digital counts are converted to spectral radiances for use in the analysis of the lunar measurements. There are factors in the performance of the instrument, such as the temperatures of the focal planes and side-to-side differences in the reflectance of the half-angle mirror, that are part of the counts-to-spectral radiance conversion for SeaWiFS.[9] The use of spectral radiances eliminates these instrumental factors from the lunar measurements.

0	0	0	0	0	0	0	0	0	0	0	0	0	0	0	0	0	0	0	0	0	0
0	0	0	0	0	0	0	0	0	0	0	0	0	0	0	0	0	0	0	0	0	0
0	0	0	0	0	0	0	0	0	1	0	0	0	0	0	0	0	0	0	0	0	0
0	0	0	0	0	0	1	0	1	1	0	0	0	0	0	0	0	0	0	0	0	0
0	0	0	0	0	1	3	9	31	23	3	1	0	0	0	0	0	0	0	0	0	0
0	0	0	0	1	3	6	35	121	92	11	4	2	0	0	0	0	0	0	0	0	0
0	0	0	1	0	4	19	146	303	267	88	4	4	1	0	0	0	0	0	0	0	0
0	0	0	0	1	7	39	232	399	359	155	7	4	1	1	1	0	0	0	0	0	0
0	0	0	0	3	10	96	351	457	471	312	41	5	5	0	1	0	0	0	0	0	0
0	0	0	1	5	14	140	378	439	481	380	76	3	5	2	1	2	1	0	0	0	0
0	0	0	1	6	26	225	382	406	462	446	166	0	7	3	2	1	1	0	0	0	0
0	0	0	1	6	36	264	379	406	445	466	222	1	8	3	3	2	2	1	0	0	0
0	0	0	1	7	60	317	393	412	402	471	291	7	8	4	2	2	0	0	0	0	0
0	0	0	2	9	78	343	416	419	391	463	305	11	8	4	2	2	2	1	0	0	0
0	0	2	2	10	99	365	442	429	394	421	327	24	7	4	2	3	1	0	1	0	0
0	0	1	4	10	107	375	450	443	412	399	330	28	6	4	3	1	1	1	0	0	0
0	0	0	3	11	120	388	441	479	472	392	322	29	7	4	3	2	1	1	1	0	0
0	0	1	3	12	118	399	433	509	514	408	318	27	6	4	3	1	1	1	1	0	0
0	0	1	4	11	113	428	434	541	581	454	300	21	8	4	2	2	1	1	0	0	0
0	0	0	3	11	101	438	440	553	606	480	293	16	8	5	3	3	2	2	0	0	0
0	0	1	4	10	69	413	492	590	630	530	272	7	8	5	3	2	2	1	1	0	0
0	0	0	4	10	52	380	540	634	635	550	234	4	9	4	3	2	2	0	0	0	0
0	0	0	2	9	32	275	603	708	642	539	149	3	9	3	3	1	2	1	1	0	0
0	0	0	1	6	24	209	599	735	638	478	94	5	7	3	3	1	1	0	0	0	0
0	0	0	1	5	15	96	435	668	555	295	32	6	4	2	2	2	1	1	0	0	0
0	0	0	1	3	12	58	317	540	436	180	14	6	3	1	1	2	1	0	1	0	0
0	0	0	0	2	7	21	115	274	213	49	7	4	2	0	1	1	0	0	0	0	0
0	0	0	0	1	5	12	48	129	96	19	5	2	1	1	1	0	1	0	0	0	0
0	0	0	0	0	1	5	10	17	13	3	1	0	0	0	1	0	0	0	0	0	0
0	0	0	0	0	1	1	3	5	3	0	0	0	0	0	0	0	0	0	0	0	0
0	0	0	0	0	0	0	1	1	0	0	0	0	0	0	0	0	0	0	0	0	0
0	0	0	0	0	0	0	1	0	0	0	0	0	0	0	0	0	0	0	0	0	0
0	0	0	0	0	0	0	0	0	0	0	0	0	0	0	0	0	0	0	0	0	0

Figure 1. A Lunar Scene as Measured by SeaWiFS. The scene is 22 samples wide by 33 scan lines long. The scene is a Mercator projection with the lunar north pole at the top. The outputs from band 1 are given as digital counts. For the analysis of lunar data, these counts are converted to spectral radiances using the SeaWiFS level 1B algorithm.

For the analysis of the lunar measurements, each scene from each band for each measurement date (such as the scene in Figure 1 for band 1 on November 14, 1997) is represented by the disk-integrated spectral radiance. Prelaunch modeling of simulated lunar images,[3] showed that disk-integrated spectral radiances produce better products than those using one, or a few, samples from the central image. In the lunar analysis, the summations (disk integrations) include all of the samples in each 22x33 sample array. They include stray light and other instrument-based optical effects. For the summations, the brightest sample in each image accounts for about 1½% to 2% of the total. For Figure 1, the brightest sample contains 735 counts, so 35 to 40 counts comprise about 0.1% of the total. The number of counts in the outer border of samples in Figure 1 is zero. For the next outer border of samples, the total number of counts is one. The use of a 22x33 sample array allows for the inclusion of all parts of the image without an excessively large number of samples of deep space.

Figure 2 shows a vertical slice through the image in Figure 1. The slice includes the counts from sample 9 for scan lines 1 through 33, that is, for samples (1,9) through (33,9). The 1% limit is used to determine the number of scan lines in each lunar image (see Section 3.4). As defined here, it is the number of scan lines within the central core of the image. This is

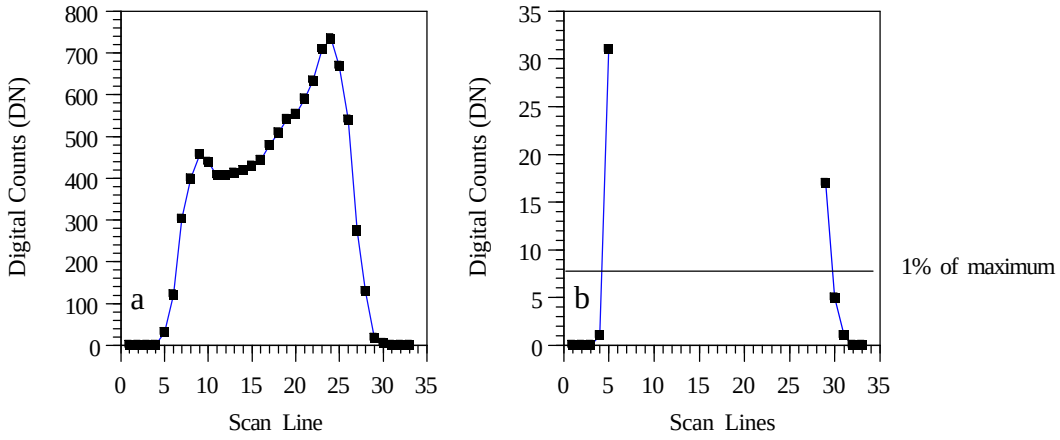

Figure 2. A Vertical Section of the Image in Figure 1. The data come from sample 9 of scan lines 1 through 33. The maximum counts in the vertical section is 735.

a. The entire vertical section.

b. An expanded view of the lowest counts in the vertical section. The horizontal line marks 1% of the maximum.

comparable to the definition of the in-band portion of the spectral responses of the SeaWiFS bands using the 1% response level.[9] As discussed below, the uncertainty in the determination of the number of scan lines in the lunar images is a major contributor to the scatter in the derived trends.

Table 2 shows the disk-integrated spectral radiances for the 9 lunar measurements. Table 3 gives the calibration coefficients used to convert counts to spectral radiances.[10] Since the moon is brighter than the surface of the ocean, lunar measurements are made with gains for the SeaWiFS bands that are less sensitive than the standard gains for Earth-viewing.

3. NORMALIZING FACTORS

The normalization factors presented here are simplified forms of the values that are calculated in the SeaWiFS level 1b algorithm. That algorithm provides calibrated radiances and geolocated Earth samples from the measurements on orbit. For example, the algorithm calculates the location of the instrument above the Earth's surface at the time of the Earth and lunar measurements. In section 3.2, each lunar measurement is assumed to occur when SeaWiFS lies on the vector between the Earth and the moon, that is, at the sub-lunar point. This assumption is also used to calculate the lunar phase angle here. The actual position of the spacecraft is calculated with much higher precision and accuracy in the level 1b algorithm. As a supplement to standard orbital calculations, the SeaStar platform also uses a Global Positioning System (GPS) receiver to determine the instrument's location. This is necessary to allow the SeaWiFS measurements of the Earth to be navigated at the single sample level (1 km at nadir). The simplified normalization factors presented here allow an examination of the components of these factors and of the magnitudes of their effects.

3.1. Sun-moon distance. For these calculations, the sun is considered to be an isotropic radiator, that is, the flux from the sun per unit solid angle is constant. As the sun-moon distance changes, the solid angle subtended by the moon also changes. When the moon is closer to the sun, it intercepts more solar flux and each point on the lunar surface becomes brighter. The effect follows the inverse square law. The normalizing factor, k_1, corrects the sun-moon distance to 1 astronomical unit (AU). It is calculated using the sun-Earth distance

$$D_{SM} = D_{SE} + \frac{R}{U} \tag{1}$$

where D_{SM} is the sun-moon distance in AU, D_{SE} is the sun-Earth distance in AU, R is the mean radius of the lunar orbit (3.844×10^5 km),[11] and U is the astronomical unit (approximately 1.4960×10^8 km).[11] The ratio, R/U, is about 0.26% of the astronomical unit. When the moon is farther from the sun, it is less bright. Thus, the normalizing factor, k_1, gives increased values with increased sun-Earth distance.

$$k_1 = \left[\frac{D_{SM}}{1\,AU}\right]^2 = \left[\frac{D_{SM}}{1}\right]^2 \tag{2}$$

Table 2. Summed Spectral Radiances for the 8 SeaWiFS Lunar Measurements. The units for the summed radiances (S) are mW cm^{-2} sr^{-1} μm^{-1}.

Date	S Band 1	S Band 2	S Band 3	S Band 4	S Band 5	S Band 6	S Band 7	S Band 8
Nov 14, 1997	412.2	494.7	572.4	572.8	605.1	583.5	517.6	409.1
Dec 14, 1997	394.1	473.1	547.7	548.1	579.6	559.4	495.4	390.3
Jan 13, 1998	399.7	479.2	554.0	554.2	584.7	561.9	496.7	389.1
Feb 10, 1998	364.8	437.7	506.7	507.6	536.3	516.3	456.5	356.5
Mar 12, 1998	345.2	414.2	479.8	480.9	507.2	488.5	431.5	335.1
Apr 12, 1998	341.1	409.5	474.1	475.2	501.6	482.1	425.3	328.9
May 12, 1998	354.2	425.4	493.0	494.0	521.6	501.4	442.1	340.4
Jun 10, 1998	379.9	455.9	528.1	528.5	557.9	535.5	471.2	361.7
Jul 10, 1998	410.5	493.3	570.8	570.9	602.2	577.3	506.2	387.7

Table 3. Prelaunch Radiometric Calibration Coefficients for the SeaWiFS Bands. The calibration constants were used to convert the counts from the lunar measurements into radiances.

SeaWiFS Band	Nominal Center Wavelength (nm)	Calibration Constant (mW cm^{-2} sr^{-1} μm^{-1} $count^{-1}$)
1	412	0.008431
2	443	0.010301
3	490	0.011889
4	510	0.011595
5	555	0.011692
6	670	0.011610
7	765	0.009630
8	865	0.008184

where the value of unity in the denominator of the factor is a reminder that k_1 is a ratio. The value of D_{SE} is derived by the SeaWiFS algorithm from a calculated ephemeris as a function of the date and time of the lunar measurement.[12] As with all of the normalizing factors used here, k_1 is dimensionless.

3.2. Instrument-moon distance. For SeaWiFS measurements, the solid angle of the moon will change with the instrument-moon distance, and for SeaWiFS measurements, the moon is larger than the field of view of the instrument. The more distant the moon from the instrument, the fewer samples it fills. As with the moon-sun distance in Section 3.1, the instrument-moon factor also varies with the square of the instrument-moon distance. The normalizing factor corrects to R, which is the average Earth-moon distance. The normalization is based on the assumption that SeaWiFS makes lunar measurements when it is at the sub-lunar point, that is, when it is on the line that connects the centers of the Earth and the moon and on the assumption that SeaWiFS has a circular orbit. This makes the instrument-moon distance shorter than that for the Earth and moon

$$D_{IM} = D_{EM} - A - H \tag{3}$$

where D_{EM} is the Earth-moon distance (in km) and D_{IM} is the instrument moon distance (in km), A is the Earth equatorial radius (6378 km),[11] and H is the instrument altitude above the Earth (705 km). The use of the instrument-moon distance in place of the Earth-moon distance has a small effect on the normalization. However, this correction is both simple and easy. The SeaWiFS level 1b algorithm performs a much more sophisticated calculation of the instrument-moon distance. Since the moon fills fewer samples when it is farther away from the Earth, the normalizing factor is larger for larger instrument-moon distances.

$$k_2 = \left[\frac{D_{IM}}{R}\right]^2 \tag{4}$$

where R is the mean radius of the lunar orbit.

3.3. Lunar phase angle. SeaWiFS views the moon once a month when the moon is about 7° from full phase. The selection of this angle is somewhat arbitrary. Because of the inclination of the moon's orbit to the plane of the Earth's orbit around the sun, there are months where the minimum phase angle for the full moon is 4°. The 7° phase angle assures the possibility of at least one lunar measurement per month and perhaps two, one with the moon approaching full phase and one with the moon leaving. The lunar phase angle effects both the moon's brightness and the fraction of the lunar surface that is illuminated when the moon is viewed from the spacecraft. These two effects are independent of each other.

Operational considerations, such as a conflict of the lunar measurement with a midnight data down link, will require the measurements to be moved to different phase angles. This occurred with the lunar measurement on January 13, 1998, where the lunar phase angle for the measurement was changed to about 5½°. SeaWiFS makes about 14½ orbits of the Earth per day. For a lunar phase cycle of 29½ days, there are about 428 SeaWiFS orbits. Since there is a change of 360° per lunar cycle, then there is a lunar phase change of about 0.8° per SeaWiFS orbit. By selecting the SeaWiFS orbit closest to 7° phase, the phase angle for each lunar measurement should be within about ½° of the desired angle.

3.3.1. Lunar reflectance. The surface of the moon is not uniformly smooth, containing mountains and craters. Regional variations of the lunar reflectance, such as variations between mare and highlands, also effect uniformity. The variation of the reflectance of the lunar surface with phase angle can be approximated by Hapke's bi-directional reflectance equation.[13] Helfenstein and Veverka[14] have used Hapke's equation, and a set of six empirically derived constants, to provide a curve of disk integrated reflectance versus phase angle. That curve is shown in Figure 3a. It is given in 1° increments from 0° to 100°. The set of coefficients used by Helfenstein and Veverka[14] are based in large part on previous measurements of the lunar albedo.[15] For our analysis, the units for reflectance in Figure 3a remain undefined. We have chosen to use a quadratic fit to provide an interpolation between the data points in Figure 3a. This interpolation scheme is limited to phase angles (θ's) between 4° and 10°.

$$f_1(\theta) = a_0 + a_1\theta + a_2\theta^2 \tag{5}$$

where a_0 is 1.287×10^{-1}, a_1 is -6.702×10^{-3}, a_2 is 2.163×10^{-4}, and θ is the phase angle The quadratic curve (see Figure 3b) agrees with the values from Figure 3a at the 0.1% level. At a phase angle of 7°, $f_1(\theta)$ is 0.09238 The normalizing factor, k_3, is calculated as a ratio

$$k_3 = \frac{f_1(7)}{f_1(\theta)} = \frac{0.09238}{a_0 + a_1\theta + a_2\theta^2} \tag{6}$$

It corrects to a value of unity at a lunar phase angle of 7°. The slopes of the curves in Figure 3a and 3b are different in sign. Thus, for phase angles less than 7°, where the reflectances are larger, k_3 makes the result smaller.

The change in lunar reflectance with phase angle from Helfenstein and Veverka[14] is monochromatic. The measurements used as a basis for their lunar reflectance model were made at wavelengths from 0.36 μm to 1.06 μm.[15] Helfenstein and Veverka[14] used the average of those measurements (over wavelength) to create a single, best-fit lunar reflectance curve at an undefined wavelength, presumably near 0.5 μm. There is an uncertainty in the use of a single lunar reflectance curve for the eight SeaWiFS bands. The refinement of this phase angle correction to account for wavelength differences will require a more refined lunar model. The other correction factors discussed here are geometric and have no wavelength dependence.

3.3.2. Lunar area. The area of the illuminated surface of the moon as seen from the Earth changes with phase angle. At 0° phase angle, the disk of the moon is fully illuminated; at 90°, half of the disk is illuminated, and at 180° phase angle, the moon is not illuminated at all. The illuminated area of the moon is a linear function of phase angle. The normalizing factor, k_4, corrects to the fractionally illuminated area of the moon at a phase angle of 7°.

$$k_4 = \frac{f_2(7)}{f_2(\theta)} \tag{7}$$

and

$$f_2(\theta) = m\theta + b \tag{8}$$

where, m=-1/180 deg^{-1}, b=1, and $f_2(7)$= 0.9611.

$$k_4 = \frac{0.9611}{m\theta + b} \tag{9}$$

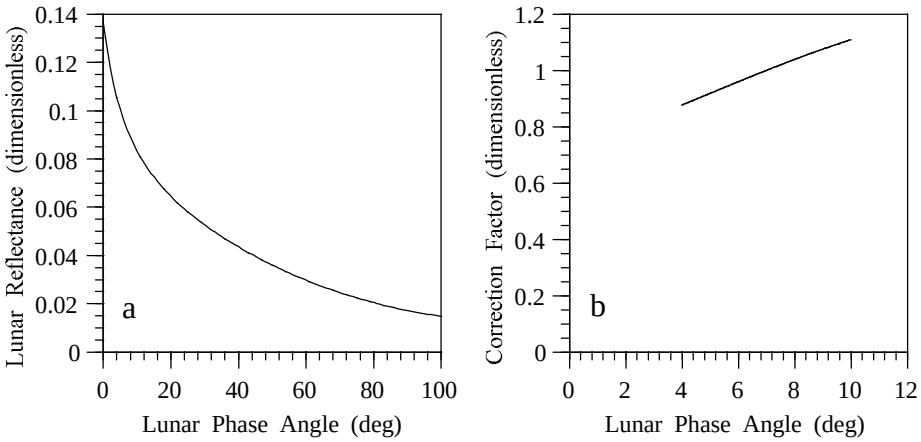

Figure 3. Disk Integrated Reflectance Versus Lunar Phase Angle.

a. The disk integrated lunar reflectance from 0° to 100° phase.
b. The Lunar Reflectance Correction Factor. The factor is calculated using Equation (6). The value at 7° phase angle is unity.

3.4. Spacecraft rotation rate. For the lunar measurements, the speed of the pitch wheels in the spacecraft is increased causing SeaWiFS to scan past the moon, which appears stationary during the measurements due to its great distance from the earth. The total number of scan lines, L_M, is calculated as the number of lines between the 1% response points for the lunar image. L_M is calculated using a vertical section of the moon, as shown in Figure 2. The scan lines of the moon are corrected to a standard, which is 25 along track scan lines with the moon at distance, R, from the Earth. The additional normalization to a standard instrument-moon distance accounts for the changes in the apparent size of the lunar disk as the distance of the moon changes. The values for R and D_{IM} are described in Section 3.2. Correction factor k_5 is calculated as

$$k_5 = \frac{25}{L_M \frac{D_{IM}}{R}} = \left[\frac{25}{L_M}\right]\left[\frac{R}{D_{IM}}\right] \qquad (10)$$

L_M is calculated as the distance (number of scan lines) between the 1% response points of the lunar image. Since the difference between 25 and 26 scan lines (or between 25 and 24) is about 4%, we use linear interpolation to increase the resolution of L_M., In addition, we calculate L_M for each band in each lunar measurement. The average of these eight L_M's (see Table 4) is used in the analysis. The standard deviations range from ½% to 1% of the averages. The measurements of L_M are made manually, examining each image individually. The values of L_M for the longest vertical sections through the images are given in Table 4.

In some measurements, where the longest vertical section passes through the center of the moon, there is a distinct difference between its length and that of the second longest vertical section. In other measurements, the two longest vertical sections are nearly equal in length. SeaWiFS images are not registered on the moon, that is, they are not aligned such that the "central" vertical section must pass through the middle of the moon. The central section in each SeaWiFS lunar image can be up to one-half pixel from the actual center. This effect has yet to be evaluated. It is anticipated to be very small.

3.5. Lunar libration. The phase angle is the most important of the geometric angular parameters for SeaWiFS lunar measurements. The variation of the integrated lunar radiance with phase angle is much stronger than any variation with libration angle. For libration changes, the loss of lunar surface from one side of the moon is balanced by the gain of visible surface on the other side. The libration effect derives from the differences in reflectance of the gained surface with respect to the surface lost. This is expected to be a strong mitigating factor for the libration effect. As with lunar reflectance versus phase angle, the effect of libration is expected to be different for different wavelengths. A detailed lunar model is required to account for lunar libration. The complete lunar libration cycle extends for 18 years. It is composed of many sub-cycles of much shorter duration. For a set of lunar measurements from several months to a few years, libration is not expected to have a major effect on the slope of the time series. It is expected to increase the scatter in the data. However, the overall contribution of libration to the SeaWiFS lunar time series remains unknown to us.

Table 4. Scan Lines in the Core of Each Lunar Image. L_M is defined as the interval between the locations where the spectral radiance is 1% of the maximum.

Date	L_M Band 1	L_M Band 2	L_M Band 3	L_M Band 4	L_M Band 5	L_M Band 6	L_M Band 7	L_M Band 8	Mean	Std Dev
Nov 14, 1997	25.71	25.79	25.63	25.92	25.36	25.83	25.25	25.56	25.63	0.22
Dec 14, 1997	25.37	25.66	25.68	25.80	24.91	25.59	24.78	25.04	25.35	0.37
Jan 13, 1998	24.53	25.06	24.78	25.37	24.00	24.84	23.92	24.07	24.57	0.50
Feb 10, 1997	24.04	24.72	24.59	25.02	23.96	24.28	23.79	23.91	24.29	0.41
Mar 12, 1998	23.63	23.88	23.87	23.98	23.41	23.79	22.94	23.50	23.62	0.32
Apr 12, 1999	23.87	24.60	24.51	24.78	23.68	24.26	23.65	23.84	24.15	0.42
May 12, 1998	25.38	26.22	25.94	26.45	25.25	25.58	25.27	25.24	25.67	0.45
Jun 10, 1998	25.98	26.63	26.30	27.00	25.83	26.07	25.65	25.86	26.17	0.43
Jul 10, 1998	26.71	26.83	26.83	26.92	26.57	26.83	26.22	26.61	26.69	0.21

Table 5. Values Used in the Calculation of the Normalizing Factors.

Date	D_{SE} (AU)	D_{EM} (km)	θ (deg)	L_M (dimensionless)
Nov 14, 1997	0.9892	368,300	6.75	25.63
Dec 14, 1997	0.9843	378,900	7.03	25.35
Jan 13, 1998	0.9835	390,000	5.45	24.57
Feb 10, 1998	0.9869	397,100	6.65	24.29
Mar 12, 1998	0.9937	404,200	6.72	23.62
Apr 12, 1998	1.0025	405,700	6.66	24.15
May 12, 1998	1.0102	401,000	7.10	25.67
Jun 10, 1998	1.0153	392,700	6.43	26.17
Jul 10, 1998	1.0166	382,100	5.70	26.69

Table 6. Normalizing Factors for the Lunar SeaWiFS Measurements. These factors are dimensionless, as are their product.

Date	k_1 (Eqn. 2)	k_2 (Eqn. 4)	k_3 (Eqn. 6)	k_4 (Eqn. 9)	k_5 (Eqn. 10)	Product
Nov 14, 1997	0.9836	0.8830	0.9900	0.9985	1.0380	0.8912
Dec 14, 1997	0.9739	0.9356	1.0011	1.0002	1.0192	0.9299
Jan 13, 1998	0.9723	0.9923	0.9369	0.9911	1.0219	0.9155
Feb 10, 1998	0.9791	1.0300	0.9859	0.9980	1.0141	1.0062
Mar 12, 1998	0.9926	1.0673	0.9888	0.9984	1.0245	1.0714
Apr 12, 1998	1.0102	1.0759	0.9863	0.9980	0.9980	1.0677
May 12, 1998	1.0257	1.0501	1.0039	1.0006	0.9493	1.0271
Jun 10, 1998	1.0361	1.0063	0.9771	0.9967	0.9525	0.9671
Jul 10, 1996	1.0387	0.9518	0.9472	0.9925	0.9601	0.8924

3.6. Combined normalization. Each normalizing factor is dimensionless and multiplicative. The combination of the correction factors is applied as

$$S_{CORR} = S\left[\frac{D_{SM}}{1}\right]^2\left[\frac{D_{IM}}{R}\right]^2\left[\frac{0.09238}{a_0 + a_1\rho + a_2\rho^2}\right]\left[\frac{0.9611}{m\rho + b}\right]\left[\frac{25}{L_M}\right]\left[\frac{R}{D_{IM}}\right] \quad (11)$$

where S is the sum from Table 2, and S_{CORR} is the sum after application of the normalizing factors. The instrument-moon distance correction occurs twice in Equation (11), once as a reciprocal in the final term. This allows a simplification of the equation to give

$$S_{CORR} = S\left[\frac{D_{SM}}{1}\right]^2\left[\frac{D_{IM}}{R}\right]\left[\frac{0.09238}{a_0 + a_1\rho + a_2\rho^2}\right]\left[\frac{0.9611}{m\rho + b}\right]\left[\frac{25}{L_M}\right] \quad (12)$$

The terms in each multiplicative fraction contain a reference constant. The variables in Equation (11) are the moon-sun distance, the instrument-moon distance, the phase angle of the moon, and the number of scan lines in the image. The moon sun distance, D_{MS}, is derived from the Earth-sun distance, D_{EM}, using Equation (1), and the instrument-moon distance, D_{IM}, is calculated from the Earth-moon distance, D_{EM}, using Equation (3).

The variable for lunar phase angle appears twice in equation (11), but the effects are not correlated, since one involves the reflectance of the lunar surface and the other the amount of the lunar surface seen by the instrument. The input variables for the correction factors are listed in Table 5. Table 6 gives the five individual normalizing factors derived from those variables. Table 6 also gives the combined normalizing factor, which is the product of the individual factors.

4. TRENDS IN SeaWiFS LUNAR MEASUREMENTS

4.1. Trends in the individual bands. Figure 4 shows the trend in the SeaWiFS measurements of the moon. The data points in each panel are the values of S_{CORR} normalized to the value on November 14, 1997. S_{CORR} is calculated using Equation (11) and the values from Table 2 and Table 6. Each panel also includes a best-fit line to the data points. The linear fit has no forcing to unity at the first measurement, but in all cases the linear fit is close to unity at the first measurement. This is an indication that there is no significant curvature in the trends. To date, we have not tried a higher order fit to the data. The changes may become exponential over time, but with the current, limited data set it is not possible to distinguish between linear and exponential trends. Figure 4 also has dashed lines at the 1.01, 1.00, and 0.99 levels. These have been included to give a visual reference for 1% changes in the data and the trend lines.

There is a distinct pattern in the results in Figure 4. For each band, the fifth value (March 12, 1998) is highest above the trend line. In a like manner, the data point from January 13, 1998 lies lowest below the line. The band-to-band similarity in the pattern of these results is an indication that it is not an instrumental effect. This conclusion is also borne out by the trends in the band ratios in Section 4.2.

Three SeaWiFS bands show decreases in sensitivity over the period of the lunar measurements. A decrease in sensitivity occurs when the instrument produces fewer counts per unit radiance. For band 6, the decrease in sensitivity is about ½% for seven months. For band 7, the change is about 1½%, and for band 8, it is a "dramatic" 5% for eight months. It may be significant that the second greatest trend in the data set is that for band 7.

4.2. Trends in the band ratios. In several of its calculations, the SeaWiFS algorithm uses ratios of the spectral radiances from the SeaWiFS bands to determine geophysical products. These band ratios use relative differences between bands, rather than their absolute values, minimizing the effects of instrumental drift in the data products. The principle behind ocean color measurements is simple. The water leaving radiances from the ocean in the green portion of the spectrum do not change with chlorophyll concentration (see Figure 3 of the SeaWiFS Overview[16]). SeaWiFS band 5, at 555 nm, measures in the green. However, the water leaving radiances in the blue region vary inversely with the chlorophyll concentration in the surface waters. The SeaWiFS algorithm can use measurements from two blue bands, band 2 at 443 nm and band 3 at 490 nm to provide the blue spectral radiances. Basically, SeaWiFS provides blue/green color ratios, or the band2/band5 and band3/band 5 spectral radiance ratios to determine ocean chlorophyll amounts. The relationship between the color ratios and the chlorophyll concentration are empirically determined.[17,18] There are semi-analytical models of the relationship, but, currently, empirical models derived from ship-board measurements give better results.

Figure 5 shows the trends in spectral radiance ratios from the lunar measurements relative to band 5. The band ratios are normalized to unity for the November 14, 1997 measurement. The plots in Figure 5 are set up in the same way as those in Figure 4 - with identical ordinates and abscissas and with identically derived trend lines. For the band ratios for bands 1 through 4, there is no trend (relative to band 5) over eight months at the 0.2% level. In addition, there is very little structure in the individual results about the trend line for any of the bands. This is an indication that much of the scatter in Figure 4, and possibly the slight downward trends in bands 1 through 5 in Figure 4, come from the correction factors in Section 3. Since band 5 shows little change with time in Figure 4, the trends in the band ratios for bands 6, 7, and 8 in Figure 5 are close to those for these bands in Figure 4.

Another ratio used in the SeaWiFS algorithm is that of the output of band 7 (765 nm) to that from band 8 (865 nm). This value in the SeaWiFS atmospheric correction is called epsilon (ε).[19] The effects of instrument-based radiometric errors on the SeaWiFS atmospheric correction have been described in the review paper by Gordon.[20] The change in the band 7 - band 8 ratio is shown in Figure 6. It is about 3% for the eight month measurement interval. This change is less than the

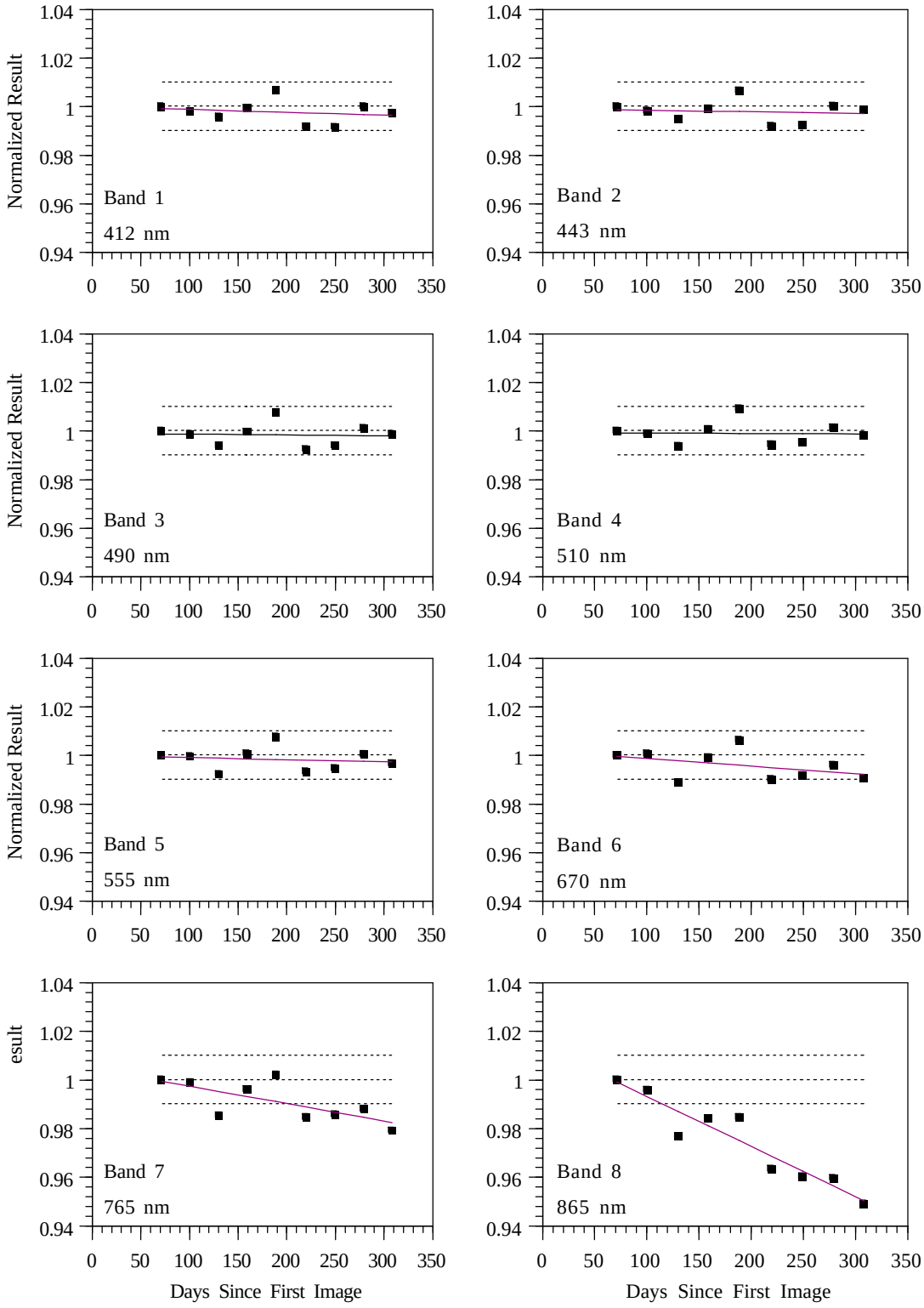

Figure 4. Changes in Instrument Response from the Lunar Measurements. For each band, these are the values of S_{CORR} normalized to the value on November 14, 1997. S_{CORR} is calculated using Equation (11) and the values from Table 2 and Table 6.

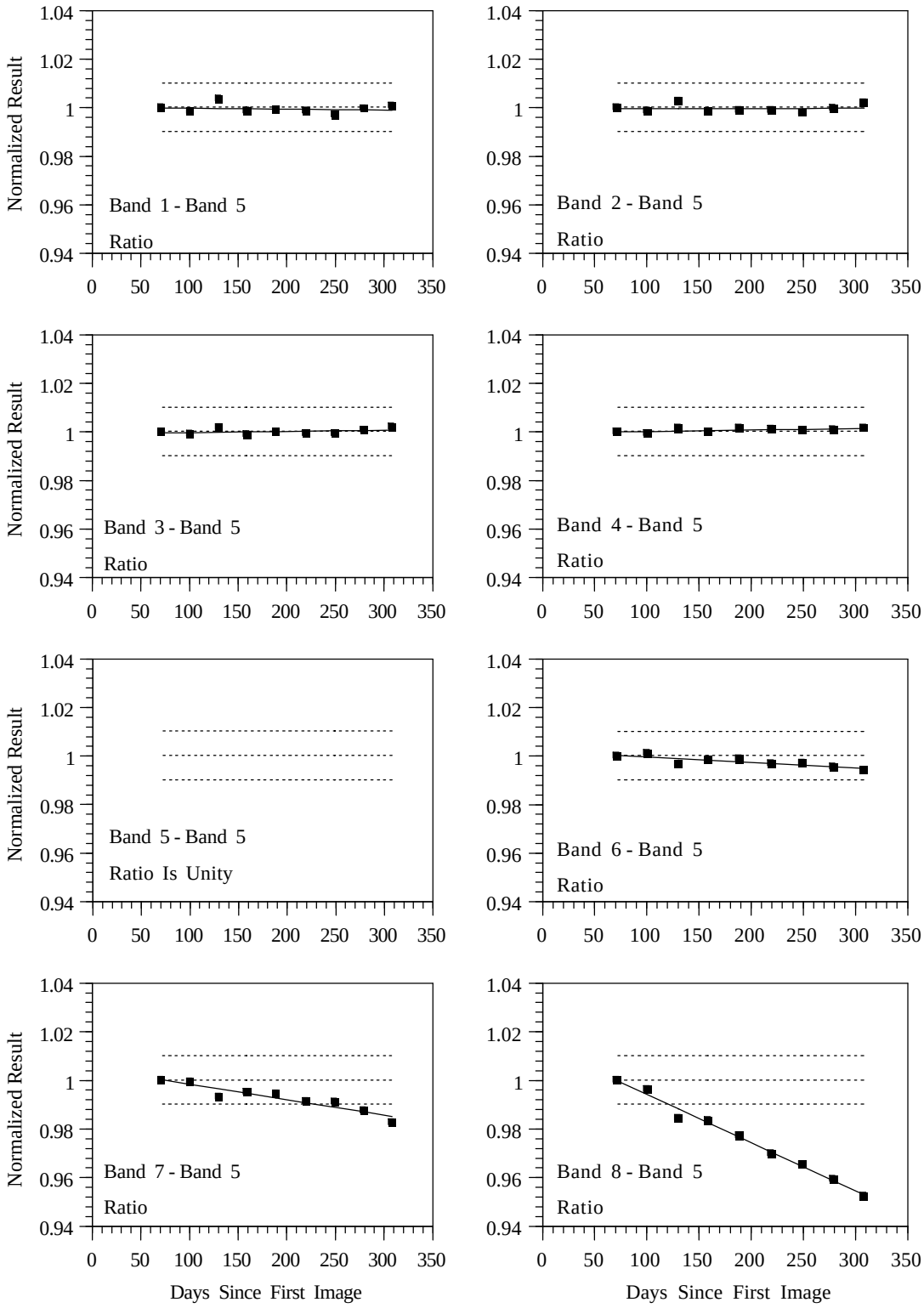

Figure 5. Changes in the Band Ratios from SeaWiFS Measurements. The ratios are given relative to band 5 (555 nm), the green band used in the determination of chlorophyll *a*.

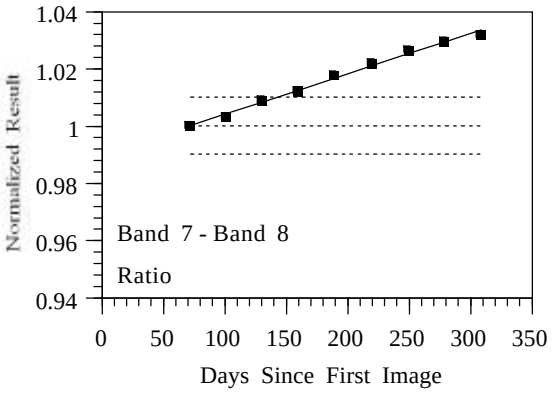

Figure 6. Changes in the Band Ratio Used to Determine Epsilon (ε) in the SeaWiFS Atmospheric Correction Algorithm. This is the ratio of the output of band 7 (765 nm) to that of band 8 (865 nm).

change for band 8 alone, since the sensitivity of band 7 is also changing, but at a lesser rate (see Figure 4). In a similar manner, the time series for epsilon in the SeaWiFS ocean measurements shows a linear increase of about 3% over the period of the lunar time series. The change in ε from the ocean measurements is roughly linear with time. The trend in the band 7 - band 8 ratio in the lunar measurements mirrors the change in ε from the ocean measurements closely. A correction for this trend in epsilon is part of the SeaWiFS data processing algorithm.

5. CONCLUDING REMARKS

The scatter in the data points around the trend lines is summarized in Table 7. The scatter in the trends for the individual bands in Figure 4 is given as the standard deviation, σ_B, in Table 7, and the scatter for the band ratios in Figures 5 and 6 is given as σ_R. For the individual bands, the values of σ_B are about ½%. For the band ratios the values of σ_R are nearly a factor of four smaller. This is an indication that the bulk of the measurement to measurement variability in the derived trends is not instrumentally caused.

Table 8 gives the estimated annual trends in the SeaWiFS measurements. These annual trends are based on the nine monthly measurements presented here. The estimates include the assumption that there is no change in the sensitivities of SeaWiFS bands 1 through 5. The annual rate of change for these bands, as shown in Figure 4, is about % per year, which may derive from imperfections in the correction factors. As a result, the values for Δ_B and the associated values for Δ_R in Table 5 are the same. The annual trend in the ratio of band 7 to band 8 is about ½% per year. It is assumed that, in the future, these trends will decrease, approaching zero change in a manner that is approximately exponential with time.

For this study, we have not corrected for the libration of the moon. Such a correction requires a model of the lunar surface.[7] However, for an extended time series, one that includes a significant portion of the libration cycle, the effect becomes an increase in scatter of the measurements in the time series. However, this may not be the principal source of the scatter in the lunar trends presented here

The determination of the number of scan lines (L_M) in the images also adds to the scatter. Originally, L_M was defined as the full width at half maximum (FWHM) of the image. In that case, L_M was calculated as the distance between the 50% response points of the images. The FWHM calculations gave measurement to measurement differences in the individual trend values that differed by 3% or more. The 50% response points occur in a portion of the image where there is a large change in spectral radiance from scan line to scan line. Presumably, this makes the calculation of L_M sensitive to measurement effects, such as the instrument's modulation transfer function[21] and the jitter in the pitch rate of the spacecraft. The use of L_M's calculated at the 1% response points cause measurement to measurement differences in the derived trend values from Table 7 that are a factor of three smaller than those based on the FWHM. The optimum method for calculating L_M remains to be determined.

This study is part of a continuing collaboration with Hugh Kieffer of the US Geologic Survey in Flagstaff, Arizona. The lunar observations from Flagstaff[22] are being used to develop a detailed lunar model that accounts for the effects of lunar libration and of the phase angle on the reflectance of the lunar surface.

Table 7. Scatter in the Data Around the Trend Lines. The scatter is described using standard deviations. The standard deviations for the bands in Figure 4 are listed as σ_B. The standard deviations for the band ratios in Figures 5 and 6 are listed as σ_R.

Band	σ_B (%)	Band Ratio	σ_R (%)
Band 1	0.43	Band 1 - Band 5	0.17
Band 2	0.42	Band 2 - Band 5	0.16
Band 3	0.44	Band 3 - Band 5	0.10
Band 4	0.44	Band 4 - Band 5	0.06
Band 5	0.44		
Band 6	0.51	Band 6 - Band 5	0.11
Band 7	0.55	Band 7 - Band 5	0.17
Band 8	0.54	Band 8 - Band 5	0.16
		Band 7 - Band 8	0.10

Table 8. Annual trends in the Sensitivities of the SeaWiFS Bands Derived from Lunar Measurements. The sensivities of bands 1 through 5 are assumed to be constant. This makes the change rates for the bands (Δ_B) the same as the change rates for the band ratios (Δ_R). The rate of change for the band7/band8 ratio is about 5% per year, since the sensitivities of bands 7 and 8 are both decreasing.

Band	Δ_B (% per year)	Band Ratio	Δ_R (% per year)
Band 1	0.0	Band 1 - Band 5	0.0
Band 2	0.0	Band 2 - Band 5	0.0
Band 3	0.0	Band 3 - Band 5	0.0
Band 4	0.0	Band 4 - Band 5	0.0
Band 5	0.0		
Band 6	0.8	Band 6 - Band 5	0.8
Band 7	2.3	Band 7 - Band 5	2.3
Band 8	7.2	Band 8 - Band 5	7.2
		Band 7 - Band 8	5.2

6. ACKNOWLEDGMENT

This study was supported by the SeaWiFS Calibration and Validation Program under Contract NAS-5-32377.

7. REFERENCES

1. Butler, J. J., and R. A. Barnes, "Calibration Strategy for the Earth Observing System (EOS) AM-1 Platform," TGARS, 36, 1056-1061, 1998.
2. McClain, C. R., W. E. Esaias, W. Barnes, B. Guenther, D. Endres, S. B. Hooker, G. Mitchell, and R. Barnes, Calibration and Validation Plan for SeaWiFS, NASA TM 104566, vol. 3, 41 pp., 1992.
3. Woodward, R. H., R. A. Barnes, C. R. McClain, W. E. Esaias, W. L. Barnes, and A. T. Mecherikunnel, Modeling of the SeaWiFS Solar and Lunar Observations, NASA TM 104566, Vol. 10, 26 pp., 1993.
4. Barnes, R. A., and A. W. Holmes, "Overview of the SeaWiFS Ocean Sensor," SPIE, 1939, 224-232, 1993.
5. Palmer, J. M., and P. N. Slater, "A Ratioing Radiometer for Use with a Solar Diffuser," SPIE, 1493, 106-117, 1991.
6. Kieffer, H. H., "Photometric Stability of the Moon," Icarus, 130, 323-327, 1997.
7. Kieffer, H. H., and R. L. Wildey, "Establishing the Moon as a Spectral Radiance Standard," J. Atmos. Oceanic Technol., 13, 360-375, 1996.
8. Barnes, R. A., A. W. Holmes, and W. E. Esaias, Stray Light in the SeaWiFS Radiometer, NASA TM 104566, Vol. 31, 76 pp., 1995.
9. Barnes, R. A., A. W. Holmes, W. L. Barnes, W. E. Esaias, C. R. McClain, and T. Svitek, SeaWiFS Prelaunch Radiometric Calibration and Spectral Characterization, NASA TM 104566, Vol. 23, 55 pp., 1994.

10. Johnson, B. C., R. E. Eplee, R. A. Barnes, E. A. Early, and R. T. Caffrey, The 1997 Prelaunch Radiometric Calibration of SeaWiFS, SeaWiFS Postlaunch TM Series, in press, 1998.
11. Seidelman, P. K., ed. Explanatory Supplement to the Astronomical Almanac, University Science Books, Mill Valley, California, 752 pp., 1992.
12. Van Flandern, T. C., and Pulkkinen, I. F., "Low-Precision Formulae for Planetary Positions," Astrophys. J. Supplement Series, 41, 391-411, 1979.
13. Hapke, B, Theory of Reflectance and Emittance Spectroscopy, New York, Cambridge University Press, 455 pp., 1993.
14. Helfenstein, P. and J. Veverka, "Photometric Properties of Lunar Terrains Derived from Hapke's Equation," Icarus, 72, 342-357, 1987.
15. Lane, A. P., and W. M. Irvine, "Monochromatic Phase Curves and Albedos for the Lunar Disk," Astron. J., 78, 267-277, 1973.
16. Hooker, S. B., W. E. Esaias, G. C. Feldman, W. W. Gregg, and C. R. McClain, An Overview of SeaWiFS Ocean Color, NASA TM 104566, Vol. 1, 25 pp., 1992.
17. Carder, K. L., S. K. Hawkes, K. A. Baker, R. C. Smith, R. G. Steward, and B. G. Mitchell, "Reflectance Model for Quantifying Chlorophyll *a* in the Presence of Productivity Degradation Products," J. Geophys. Res., 96, 20,559-20,611, 1991.
18. Aiken, J., G. F. Moore, C. C. Trees, S. B. Hooker, and D. K. Clark, The SeaWiFS CZCS-Type Pigment Algorithm, NASA TM 104566, Vol. 29, 34 pp., 1995.
19. Gordon H. R., and M. Wang, "Retrieval of Water-Leaving Radiance and Aerosol Optical Thickness over the Oceans with SeaWiFS: A Preliminary Algorithm," Appl. Opt., 33, 443-452, 1994.
20. Gordon, H. R., "Atmospheric Correction of Ocean Color Imagery in the Earth Observing System Era," J. Geophys. Res., 102, 17,081-17,106, 1997.
21. Barnes, R. A., W. L. Barnes, W. E. Esaias, and C. R. McClain, Prelaunch Acceptance Report for the SeaWiFS Radiometer, NASA TM 104566, Vol. 22, 32 pp., 1994.
22. Kieffer, H. H., and J. M. Anderson, "Use of the Moon for Spacecraft Calibration over 350-2500 nm," these proceedings, 1998.